Metabolic Engineering 13 (2011) 353–363

Contents lists available at ScienceDirect

Metabolic Engineering

journal homepage: www.elsevier.com/locate/ymben

Metabolic engineering of cyanobacteria for 1-butanol production from carbon dioxide

Ethan I. Lan [a,b], James C. Liao [a,b,*]

[a] Department of Chemical and Biomolecular Engineering, University of California, Los Angeles, CA 90095, USA
[b] Biomedical Engineering IDP, University of California, Los Angeles, CA 90095, USA

ARTICLE INFO

Article history:
Received 8 March 2011
Received in revised form
25 April 2011
Accepted 28 April 2011
Available online 4 May 2011

Keywords:
Cyanobacteria
Butanol
Biofuel
Metabolic engineering
Synthetic biology

ABSTRACT

Production of chemicals and fuels directly from CO_2 is an attractive approach to solving the energy and environmental problems. 1-Butanol, a chemical feedstock and potential fuel, has been produced by fermentation of carbohydrates, both in native *Clostridium* species and various engineered hosts. To produce 1-butanol from CO_2, we transferred a modified CoA-dependent 1-butanol production pathway into a cyanobacterium, *Synechococcus elongatus* PCC 7942. We demonstrated the activity of each enzyme in the pathway by chromosomal integration and expression of the genes. In particular, *Treponema denticola* trans-enoyl-CoA reductase (Ter), which utilizes NADH as the reducing power, was used for the reduction of crotonyl-CoA to butyryl-CoA instead of *Clostridium acetobutylicum* butyryl-CoA dehydrogenase to by-pass the need of *Clostridial* ferredoxins. Addition of polyhistidine-tag increased the overall activity of Ter and resulted in higher 1-butanol production. Removal of oxygen is an important factor in the synthesis of 1-butanol in this organism. This result represents the first autotrophic 1-butanol production.

1. Introduction

While lignocellulose and sugars have been the major source of carbon for microbial production of biofuels (Atsumi and Liao, 2008; Fischer et al., 2008; Zhang et al., 2008), direct conversion of CO_2 to fuel using photoautotrophic organisms, such as cyanobacteria, has received increasing attention. The readily available genetic tools and genome sequences make cyanobacteria a favored target of metabolic engineering for producing desired products (Fig. 1A). For example, cyanobacteria have been demonstrated to produce isobutyraldehyde (1100 mg/L), isobutanol (450 mg/L) (Atsumi et al., 2009), ethanol (0.021–550 mg/L) (Deng and Coleman, 1999; Dexter and Fu, 2009), ethylene (~37 mg/L) (Takahama et al., 2003), isoprene (0.05 mg/g dry cell/day) (Lindberg et al., 2010), sugars (~36 mg/L), and lactic acid (~56 mg/L) (Niederholtmeyer et al., 2010). The relatively high-flux production of isobutanol and isobutyraldehyde (Atsumi et al., 2009; Sheehan, 2009) demonstrates the feasibility for commercial scale synthesis from CO_2.

1-Butanol is considered as a potential fuel substitute to displace gasoline. The energy density of 1-butanol (27 MJ/L) is higher than that of ethanol (21 MJ/L) and closer to that of gasoline (32 MJ/L). In addition, its low hygroscopicity and compatibility with current infrastructure make 1-butanol an attractive fuel substitute. 1-Butanol is also an important feedstock used to produce various chemicals. To produce one molecule of 1-butanol using photosynthesis and the Calvin–Benson cycle, 48 photons are required (see Box 1). This photon yield is the same as glucose and isobutanol, and compares favorably to other chemicals such as isoprene and ethylene (Table 1). Therefore, it is desirable to produce 1-butanol directly from CO_2 and light.

1-Butanol can be produced via two distinct pathways. The synthetic 2-ketoacid pathway utilizes intermediates from amino acid biosynthesis routes (Atsumi et al., 2008b; Shen and Liao, 2008). 2-ketovalerate, a non-natural intermediate produced by the enzymes LeuABCD of leucine biosynthesis, is decarboxylated and then reduced to 1-butanol. The other pathway synthesizes butyryl-CoA from acetyl-CoA in a pathway similar to fatty acid biosynthesis. Butyryl-CoA is then reduced to 1-butanol. This pathway is referred to as the CoA-dependent pathway and is used in nature by various *Clostridium* species to produce 1-butanol along with ethanol and acetone.

Among *Clostridium* species, *Clostridium acetobutylicum* and *Clostridium beijerinckii* have been used to ferment carbohydrates into 1-butanol (Ezeji et al., 2004; Lin and Blaschek, 1983) with increased butanol tolerance (Nicolaou et al., 2010) and selectivity over by-products (Jiang et al., 2009; Sillers et al., 2008). As an alternative, various groups have produced 1-butanol using the CoA-dependent

* Corresponding author at: Department of Chemical and Biomolecular Engineering, University of California, 5531 Boelter Hall, 420 Westwood Plaza, Los Angeles, CA 90095, USA. Fax: +1 310 206 4107.
E-mail address: liaoj@seas.ucla.edu (J.C. Liao).

1096-7176/$ - see front matter © 2011 Elsevier Inc. All rights reserved.
doi:10.1016/j.ymben.2011.04.004

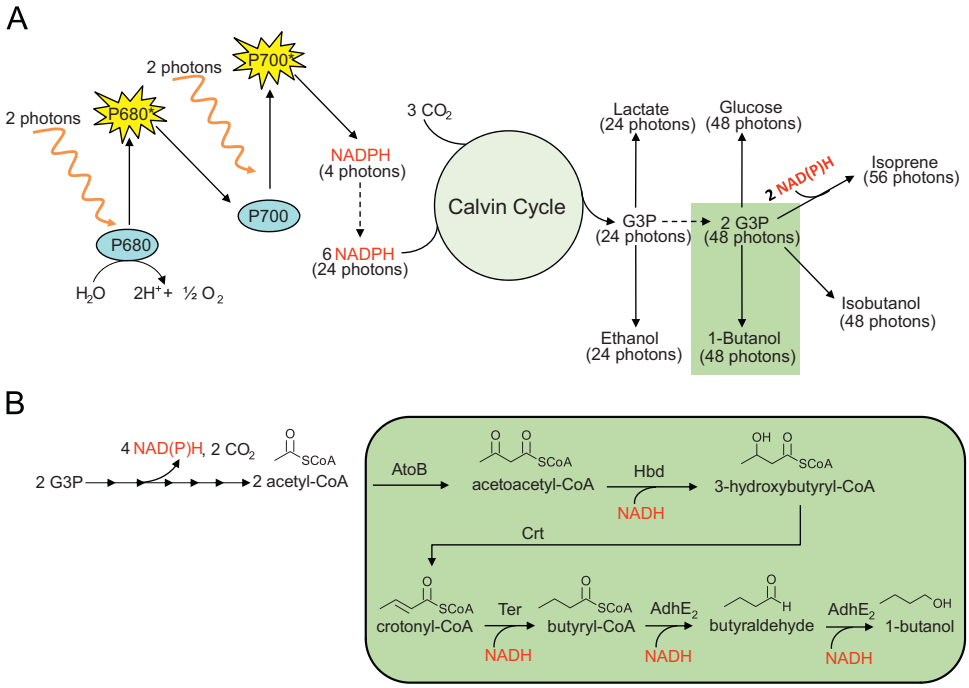

Fig. 1. Schematic representation of 1-butanol production in engineered *S. elongatus* PCC 7942. (A) Light reaction provides NADPH as the reductant for carbon fixation into bioproducts. Photons required to produce each product is calculated based on the number of glyceraldehydes-3-phosphate (G3P) and NAD(P)H required. (B) The engineered *S. elongatus* 7942 contains heterologous expression of five enzymes for the conversion of acetyl-CoA to 1-butanol (boxed in green): AtoB, acetyl-CoA acetyltransferase; Hbd, 3-hydroxybutyryl-CoA dehydrogenase; Crt, crotonase; Ter, trans-2-enoyl-CoA reductase; and AdhE2, bifunctional aldehyde/alcohol dehydrogenase. (For interpretation of the references to color in this figure legend, the reader is referred to the web version of this article.)

Box 1–Maximum theoretical yield of 1-butanol

On average, **200 W/m^2** of solar energy is available on earth (Brenner et al., 2008). This equals to **6.32×10^6 kJ/m^2/yr**. However, only a fraction of the total solar energy can be utilized by photosynthetic organisms. The energy used for carbon fixation is limited by photosynthetically inactive spectrum (Zhu et al., 2008) (51.3% loss of total energy), light reflected and transmitted (green is reflected, 4.9%), photochemical inefficiency (as a result of energy lost by relaxation of higher excitation state of chlorophyll, 6.6%), photorespiration (6.1%), and respiration (1.9%). Therefore, only **29.2%**, corresponding to **1.85×10^6 kJ/m^2/yr**, of the solar irradiation can be used by photosynthetic machinery to produce biological compounds.

48 moles of photons (of energy 173.5 kJ/mol, representing the average energy of 680 and 700 nm photons) are required to make one mole of 1-butanol (Fig. 1A). This photon yield is calculated by the number of photons needed to fix CO_2 into glyceraldehyde-3-phosphate (G3P) and then the number of G3P and NAD(P)H required to produce 1-butanol. 2 photons (one from each photosystem) are required to transfer 1 electron from H_2O to $NADP^+$. Production of NADPH from $NADP^+$ requires two electrons. Therefore 4 photons are required to produce 1 NADPH. 6 NADPH are required to produce 1 G3P from 3 CO_2. Thus 24 photons are required for producing G3P. To produce 1-butanol, 2 G3P are required, which is equal to 48 photons.

Therefore, **8328 kJ** is required to produce 1 mole of 1-butanol. Taking the total energy available for producing compounds (**1.85×10^6 kJ/m^2/yr),** divided by **8328 kJ/mol** yields **221 mol/m^2/yr**, or **16 kg/m^2/yr**, of 1-butanol can be produced.

Table 1

Compound	Photons required	Maximum yield (kg/m^2/yr)
Ethanol	24	20.5
Lactate	24	40.0
Glucose	48	40.0
Ethylene	48	6.2
1-Butanol	**48**	**16.5**
Isobutanol	48	16.5
Isoprene	56	13.0

pathway by non-native hosts, including *Escherichia coli* (550–1200 mg/L) (Atsumi et al., 2008a; Inui et al., 2008; Nielsen et al., 2009), *Saccharomyces cerevisiae* (2.5 mg/L) (Steen et al., 2008), *Lactobacillus brevis* (300 mg/L) (Berezina et al., 2010), *Pseudomonas putida* (120 mg/L), and *Bacillus subtilis* (24 mg/L) (Nielsen et al., 2009). The related pathway for production of isopropanol has also been transferred to *E. coli* (Hanai et al., 2007). The native *Clostridium* 1-butanol formation pathway consists of seven enzymes: thiolase (Thl), 3-hydroxybutyryl-CoA dehydrogenase (Hbd), crotonase (Crt), butyryl-CoA dehydrogenase (Bcd), electron transferring proteins A and B (EtfAB), and bifunctional aldehyde alcohol dehydrogenase (AdhE2). In particular, Bcd/EtfAB catalyzes the hydrogenation of crotonyl-CoA to butyryl-CoA and is coupled to ferredoxin reduction (Li et al., 2008). This enzyme complex has not been expressed well in heterologous hosts and is oxygen sensitive (Atsumi et al., 2008a; Berezina et al., 2010; Boynton et al., 1996; Inui et al., 2008; Nielsen et al., 2009). In addition, Bcd/Etf complex may require *Clostridial* ferredoxins to function at its optimum. Recently Shen et al. (2011) obtained high yield (88% of theoretical) and high flux production with an effective titer up to 30 g/L of 1-butanol in *E. coli* by both streamlining carbon flux and reducing cofactors using

acetyl-CoA and NADH driving forces coupled with the NADH-dependent trans-enoyl-CoA reductase (Ter) (Tucci and Martin, 2007). The use of Ter effectively avoids the problems of expressing *Clostridium* Bcd/EtfAB complex as well as by-passing the need for expressing *Clostridial* ferredoxins.

No reports thus far have engineered autotrophic organisms to produce 1-butanol. Expression of the CoA-dependent pathway is challenging for cyanobacteria in many aspects. Since this pathway is derived from strict anaerobes, expressing such a pathway into cyanobacteria, which produce oxygen during photosynthesis, is challenging as enzymes involved may be negatively affected by the presence of oxygen. In addition, heterologous protein expression requires careful modulation. Unfortunately, the ability to control gene expression in cyanobacteria is limited. In this article, we successfully express all of the genes in the CoA-dependent 1-butanol pathway in *Synechococcus elongatus* 7942 and achieved 1-butanol production from CO_2 and light. We introduce (Fig. 1B) *hbd*, *crt*, and *adhE2* genes from *C. acetobutylicum*, the *ter* gene from *Treponema denticola*, and the *atoB* gene from *E. coli* into wild-type *S. elongatus* 7942. AtoB is selected for this work because it has been demonstrated to outperform Thl in previous *E. coli* results (Atsumi et al., 2008a Shen et al., 2011). In addition, AtoB (Duncombe and Frerman, 1976) has been shown with higher specific activity (1078 U/mg) when compared to Thl (216 U/mg) (Wiesenborn et al., 1988). Interestingly, polyhistidine-tag increases the expression of T.d-Ter, which enhances 1-butanol production. Inhibiting the cyanobacteria's oxygen evolving capability after growth, we demonstrate the first production of 1-butanol in cyanobacteria.

2. Materials and methods

2.1. Chemicals and reagents

All chemicals were purchased from Sigma-Aldrich (St. Louis, MO) or Fisher Scientifics (Pittsburgh, PA) unless otherwise specified. B-PERII protein extraction reagent was purchased from Thermo Scientific (Rockford, IL). iProof high-fidelity polymerase, SDS-Page gel, and Bradford reagent were purchased from Bio-Rad (Hercules, CA). Restriction enzymes, phusion DNA polymerase, and ligases were purchased from New England Biolabs (Ipswich, MA). T5-Exonuclease was purchased from Epicentre Biotechnologies (Madison, WI). Lysonase™ was purchased from EMD Biosciences (San Diego, CA).

2.2. Culture medium and condition

All *S. elongatus* 7942 strains were grown on modified BG-11 (1.5 g/L $NaNO_3$, 0.0272 g/L $CaCl_2$, 0.012 g/L ferric ammonium citrate, 0.001 g/L Na_2EDTA, 0.040 g/L K_2HPO_4, 0.0361 g/L $MgSO_4$, 0.020 g/L Na_2CO_3, 1000 × trace mineral (1.43 g H_3BO_3, 0.905 g/L $MnCl_2 \cdot 4H_2O$, 0.111 g/L $ZnSO_4 \cdot 7H_2O$, 0.195 g/L $Na_2MoO_4 \cdot 2H_2O$, 0.0395 g $CuSO_4 \cdot 5H_2O$, 0.0245 g $Co(NO_3)_2 \cdot 6H_2O$), and 0.00882 g/L sodium citrate (Bustos and Golden, 1991)) agar (1.5% w/v) plates. All *S. elongatus* 7942 strains were cultured in BG-11 medium (Sigma-Aldrich) containing 50 mM $NaHCO_3$ either in shake flasks, screw-capped flasks, or Roux culture bottles. Cultures were grown under 150 μE/s/m^2 light condition at 30 °C. Cell growth was monitored by measuring OD_{730} with Beckman-Coulter DU-800 spectrophotometer.

2.3. DNA manipulations

All chromosomal manipulations were carried out by recombination of plasmid DNA into *S. elongatus* 7942 genome at neutral site I (NSI) (Bustos and Golden, 1992) and neutral site II (NSII) (Andersson et al., 2000). Unless specified otherwise, all plasmid were constructed using the isothermal DNA assembly method (Gibson et al., 2009). Plasmids were constructed in *E. coli* XL-1 strain for propagation and storage (Table 2). Genes *atoB* and *adhE2* were cloned from pJCL17 (Atsumi et al., 2008a). Genes *crt* and *hbd* were cloned from pEL11 (Shen et al., 2011), and *T. denticola ter* (hereforth referred to as *T.d-ter.*) was cloned from pIM8 (Shen et al., 2011). Poly-His-tagged *T.d-ter* (His-*T.d-ter*) was cloned from an expression vector containing this gene that was cloned previously by inserting the T.d-*ter* gene from pIM8 into pCDFduet plasmid (Novagene) between the BamHI and SalI sites. His-tagged *Euglena gracilis ter* (henceforth referred to as His-*E.g-*

Table 2
Strains and plasmids used.

Strain	Relevant genotypes	Reference
PCC 7942	Wild-type	S.S. Golden
EL1	*atoB, adhE2* integrated at NSI and *T.d-ter, crt, hbd* integrated at NSII in PCC 7942 genome	This work
EL7	*atoB, adhE2* integrated at NSI and ter_{op} (optimized for *S. elongatus* 7942), *crt, hbd* integrated at NSII in PCC 7942 genome	This work
EL9	His-tagged *T. denticola ter* (His-*T.d-ter*) integrated at NSI in PCC 7942 genome	This work
EL10	His-tagged *E. gracilis ter* (His-*E.g-ter*) integrated at NSI in PCC7943 genome	This work
EL11	His-tagged *C. acetobutylicum hbd* (His-*hbd*) integrated at NSI in PCC7944 genome	This work
EL13	*atoB, adhE2, T.d-ter, hbd, crt* integrated at NSI in PCC 7942 genome	This work
EL14	His-*T.d-ter* integrated at NSI and *atoB, adhE2, crrt, hbd* integrated at NSII in PCC 7942 genome	This work
Plasmid	***Genotypes***	
pCDFduet	Spec^R; plasmid containing poly-His tag	Novagen
pAM2991	Spec^R; NSI targeting vector; Ptrc	Bustos and Golden (1991)
pYX35	Kan^R; NSII targeting vector; PLlacO1::*rbcL, rbcS*	Yixin Huo (unpublished)
pJCL17	Amp^R; ColE1 ori; $P_L lacO_1$::*atoB, adhE2*	Atsumi et al. (2008a, 2008b)
pEL11	Amp^R; ColE1 ori; $P_L lacO_1$::*atoB, adhE2, crt, hbd*	Shen et al. (2011)
pIM8	Kan^R; ColA ori; $P_L lacO_1$::T.d-*ter*	Shen et al. (2011)
pEL5	Spec^R; NSI targeting; Ptrc::*atoB, adhE2*	This work
pEL14	Kan^R; NSII targeting; $P_L lacO_1$::T.d-*ter, crt, hbd*	This work
pEL17	Spec^R; NSI targeting; Ptrc::*atoB, adhE2, PLlacO1: T.d-ter, hbd, crt*	This work
pEL19	Kan^R; NSII targeting; $P_L lacO_1$::T.d-ter_{op}, *crt, hbd*	This work
pEL30	Spec^R; NSI targeting; Ptrc::His-T.d-*ter*	This work
pEL31	Spec^R; NSI targeting; Ptrc::His-E.g-*ter*	This work
pEL32	Spec^R; NSI targeting; Ptrc::His-*hbd*	This work
pEL37	Kan^R; NSII targeting; $P_L lacO_1$::*atoB, adhE2, crt, hbd*	This work

Kan^R, kanamycin resistance; Spec^R, spectinomycin resistance; Amp^R, ampicillin resistance.

ter) and His-tagged *C. acetobutylicum hbd* (His-*hbd*) were cloned in a similar fashion. Codon optimized *T. denticola ter* (*T.d-ter*$_{op}$) for *S. elongatus* 7942 was synthesized by Genewiz Inc.

2.4. Plasmid constructions

The plasmids used and constructed in this work are listed in Table 2 and briefly described below. Plasmid pEL5 was constructed by insertion of *atoB* and *adhE2* into pAM2991, between the BamHI and NotI sites, under an IPTG-inducible promoter Ptrc. The *atoB, adhE2* fragment was amplified by PCR using primers rEL-56 and rEL-57 with pJCL17 as the template. Primer sequences are listed in Table 3.

Plasmid pEL14 was constructed by inserting a *T.d-ter, crt, hbd* fragment between BamHI and MluI sites of a digested plasmid pYX35. The *T.d-ter, crt, hbd* fragment was amplified via splicing by overlap extension (SOE) of *T.d-ter* and *crt*, *hbd* fragment using primers rEL-58 and rEL-61. The *T.d-ter* fragment was amplified using primers rEL-58 and rEL-59 with pIM8 as the template. The *crt*, *hbd* fragment was amplified with primers rEL-60 and rEL-61 using pEL11 as the template.

Plasmid pEL17 was constructed by DNA assembly of two pAM2991 (Bustos and Golden, 1991) fragments, a *T.d-ter*, *hbd*, *crt* fragment, and a $P_L lacO_1$, *atoB*, *adhE2* fragment. The two pAM2991 fragments were separately amplified with primers rEL-202 and rEL-220 for one fragment and rEL-219 and rEL-226 for the other with pAM2991 as the template. The *T.d-ter*, *hbd*, *crt* fragment was amplified by SOE of a *T.d-ter* fragment and *hbd, crt* fragment using primers rEL-176 and rEL-181. The *T.d-ter* fragment was amplified using primers rEL-176 and rEL-177 with pIM8 as the template. The *hbd*, *crt* fragment was amplified by another SOE using primers rEL-178 and rEL-181. The *hbd* fragment was amplified using primers rEL-178 and rEL-179 with pEL11 as the template as well. The *crt* fragment was amplified with primers rEL-180 and rEL-181 and pEL11 as the template.

Plasmid pEL19 was constructed by DNA assembly of a pEL14 fragment without *T.d-ter* and a codon optimized *T.d-ter* (*T.d-ter*$_{op}$) fragment. The pEL14 fragment without wild-type *T.d-ter* was amplified using primers rEL-195 and rEL-217 with pEL14 as the template. The *T.d-ter*$_{op}$ fragment was amplified with primers rEL-209 and rEL-218 and the plasmid synthesized by Genewiz Inc. as the template.

Plasmid pEL30 was constructed by DNA assembly of two pAM2991 fragments and a His-*T.d-ter* fragment. The pAM2991 fragments were amplified in the same manner as in the construction for plasmid pEL17. The His-*T.d-ter* fragment was amplified using primers rEL-192 and rEL-204 with a previously cloned pCDFduet (Novagen) plasmid containing His-*T.d-ter* as the template.

Plasmid pEL31 was constructed in a similar fashion as plasmid pEL30. It was constructed by DNA assembly of 2 pAM2991 fragments

Table 3
Primers sequences.

Primers	Sequence (5′→3′)	Used for plasmid
rEL-56	GGGAAAGGATCCATGAAAAATTGTGTCATCGTCAGTGCGG	pEL5
rEL-57	GGGAAAGCGGCCGCTTAAAATGATTTTATATAGATATCCTTAAGTTCACTTATA	pEL5
rEL-58	GGGAAAGGATCCATGATTGTAAAACCAATGGTTAGGAACAAT	pEL14
rEL-59	AGTTCCATGGTATATCTCCTCTAAATCCTGTCGAACCTTTCTACCTCG	pEL14
rEL-60	AAAGGTTCGACAGGATTTAGAGGAGATATACCATGGAACTAAACAATGTCATCC	pEL14
rEL-61	GGGAAAACGCGTTTATTTTGAATAATCGTAGAAACCTTTTCCTGATT	pEL14
rEL-176	ACAGAAGGAGACTTAAGGATCACTAGTATGATTGTAAAACCAATGGTTAGGAACAATATT	pEL17
rEL-177	CATACCTTTTTCATGGTATATCTCCTACTAGTTTAAATCCTGTCGAACCTTTCTACCTCG	pEL17
rEL-178	CAGGATTTAAACTAGTAGGAGATATACCATGAAAAAGGTATGTGTTATAGGTGCAGGTAC	pEL17
rEL-179	GGTATATCTCCTCTCGAGTTATTTTGAATAATCGTAGAAACCTTTTCCTG	pEL17
rEL-180	ATTCAAAATAACTCGAGAGGAGATATACCATGGAACTAAACAATGTCATCCTTGAAAAGG	pEL17
rEL-181	CTAAATACATTCAAATATGTCTATCTATTTTTGAAGCCTTCAATTTTTCTTTTC	pEL17
rEL-182	TTGAAGGCTTCAAAAATAGATAGACATATTTGAATGTATTTAGAAAAATAAACAAATAGG	pEL17
rEL-187	AGCATACTAGAGGATCGGCGGCCGCTTAAAATGATTTTATATAGATATCCTTAAGTTCAC	pEL17
rEL-202	CGATCCTCTAGTATGCTTGTAAACCGTTTT	pEL17, pEL30, pEL31, pEL32
rEL-219	CGGTAATACGGTTATCCACAGAATCA	pEL17, pEL30, pEL31, pEL32
rEL-220	TGATTCTGTGGATAACCGTATTACCG	pEL17, pEL30, pEL31, pEL32
rEL-226	GTGTGAAATTGTTATCCGCTCACAATTC	pEL17, pEL30, pEL31, pEL32
rEL-209	TGTTTAGTTCCATGGTATATCTCCTTTAGATGCGGTCAAAACGCTCAACC	pEL19
rEL-218	CTGACCGAATTCATTAAAGAGGAGATATACCATGATCGTAAAACCTATGGTTCGTAACAA	pEL19
rEL-195	AGGAGATATACCATGGAACTAAACAATGTCATC	pEL19
rEL-217	CTTTAATGAATTCGGTCAGTGCGTCCT	pEL19, pEL37
rEL-192	AACAATTTCACACAGGAGATATACCATGGGCAGCAGCCATCACCATCATC	pEL30, pEL31, pEL32
rEL-204	GTTTACAAGCATACTAGAGGATCGTTAAATCCTGTCGAACCTTTCTACCTCG	pEL30, pEL31, pEL32
rEL-203	GTTTACAAGCATACTAGAGGATCGTTATTGTTGAGCGGCAGAAGGCAGATCC	pEL31
rEL-205	GTTTACAAGCATACTAGAGGATCGTTATTTTGAATAATCGTAGAAACCTTTTCCTGATT	pEL32
rEL-254	AGGACGCACTGACCGAATTCATTAAAG	pEL37
rEL-255	TTTATTTGATGCCTCTAGCACGCGTTTATTTTGAATAATCGTAGAAACCTTTTCCTG	pEL37
rEL-253	ACGCGTGCTAGAGGCATCAAATAAA	pEL37
rEL-148	GGGAAAGGATCCATGAAAAATTGTGTCATCGTCAGTGCGG	N/A; *atoB* gene specific
rEL-149	GGGAAAGCGGCCGCATTAATTCAACCGTTCAATCACCATCGC	N/A; *atoB* gene specific
rEL-156	GGGAAAGGATCCATGAAAAAGGTATGTGTTATAGGTGCAGGTACTATG	N/A; *hbd* gene specific
rEL-157	GGGAAAGCGGCCGCATTATTTTGAATAATCGTAGAAACCTTTTCCTG	N/A; *hbd* gene specific
rEL-158	GGGAAAGGATCCATGGAACTAAACAATGTCATCCTTGAAAAGGA	N/A; *crt* gene specific
rEL-159	GGGAAAGCGGCCGCACTATCTATTTTTGAAGCCTTCAATTTTTCTTTTC	N/A; *crt* gene specific
rEL-160	GGGAAAGGATCCATGATTGTAAAACCAATGGTTAGGAACAAT	N/A; T.d-*ter* gene specific
rEL-161	GGGAAAGCGGCCGCATTAAATCCTGTCGAACCTTTCTACCTCG	N/A; T.d-*ter* gene specific
rEL-209	TGTTTAGTTCCATGGTATATCTCCTTTAGATGCGGTCAAAACGCTCAACC	N/A; T.d-*ter*$_{op}$ gene specific
rEL-218	CTGACCGAATTCATTAAAG AGGAGATATACC ATGATCGTAAAACCTATGGTTCGTAACAA	N/A; T.d-*ter*$_{op}$ gene specific
rEL-163	GGGAAAGCGGCCGCATTAAAATGATTTTATATAGATATCCTTAAGTTCAC	N/A; *adhE2* gene specific
rEL-adhE2-f3	TCTTAGATTTGCATTAAAAG	N/A; *adhE2* gene specific

and a His-*E.g-ter* fragment. Primers rEL-192 and rEL-203 and a pCDFduet plasmid containing His-*E.g-ter* were used for the amplification of the His-*E.g-ter* fragment.

Plasmid pEL32 was also constructed in a similar fashion as pEL30 by DNA assembly of 2 pAM2991 fragments and a His-*hbd* fragment. The His-*hbd* fragment was amplified by primers rEL-192 and rEL-205 and a pCDFduet plasmid containing His-*hbd* as the template.

Plasmid pEL37 was constructed by DNA assembly of a pEL14 backbone fragment without the *T.d-ter, crt, hbd genes* and a *atoB*, *adhE2*, *crt*, *hbd* fragment. The pEL14 backbone fragment was amplified using primers rEL-217 and rEL-253 and pEL14 as the template. The *atoB*, *adhE2*, *crt*, *hbd* fragment was amplified with primers rEL-254 and rEL-255 and pEL11 as the template.

2.5. Strain construction

The strains used and constructed are listed in Table 2. Briefly, strain EL1 was constructed by recombination of plasmids pEL5 and pEL14 at NSI and NSII of wild-type *S. elongatus* 7942, respectively (Table 2 for relevant genotypes). Strain EL7 was constructed by the recombination of plasmids pEL5 and pEL19 into wild-type *S. elongatus* 7942. Strain EL9 was constructed by recombination of plasmid pEL30 into NSI of wild-type *S. elongatus* 7942. Strain EL10 was constructed by recombination of plasmid pEL31 into NSI of wild-type *S. elongatus* 7942. Strain EL11 was constructed by recombination of plasmid pEL32 into NSI of wild-type *S. elongatus* 7942. Strain EL13 was constructed with plasmid pEL17 recombination into NSI site of wild-type *S. elongatus* 7942 genome. Strain EL14 was constructed by pEL37 recombination into a strain EL9 at NSII.

2.6. Plasmid transformation

S. elongatus 7942 strains were transformed by incubating cells at mid-log phase (OD_{730} of 0.4–0.6) with 2 μg of plasmid DNA overnight in dark. The culture was then spread on BG-11 plates with appropriate antibiotics for selection of successful recombination. For selection and culture maintenance, 20 μg/ml spectinomycin and 10 μg/ml kanamycin were added into BG-11 agar plates and BG-11 medium where appropriate. Colonies grown on BG-11 agar plates were analyzed by PCR using gene-specific primers (Table 3) to verify integration of inserted genes into the recombinant strain. In all cases, four individual colonies were analyzed by PCR for verification. One positive colony was then propagated and tested for downstream experiments.

2.7. Western blot analysis

Western blot was performed using standard procedure. 20 μg of soluble protein was separated by SDS-PAGE. Commercially available His-probe-HRP kit (Thermo Scientific) was used to detect protein expression of His-tagged *T. denticola* Ter, *E. gracilis* Ter, and *C. acetobutylicum* Hbd. Film exposure time was 5 s.

2.8. Production of 1-butanol

Seed culture was grown in 250 mL screw-cap bottle until OD_{730} reaches 1.5. The seed culture was then used to inoculate a new culture that was grown under continuous light and constant bubbling of 5% CO_2/95% N_2 in Roux culture bottle placed vertically. 1 mM IPTG was added to the culture (OD_{730} of 0.6) for gene induction. The culture was grown to OD_{730} of 3.5–4.0 at which the culture was used to test 1-butanol accumulation in various conditions and separated into different test tubes. Dark condition was accomplished by wrapping the test tubes with aluminum foil, whereas light condition was done without wrapping. Anoxic condition was introduced by purging the head-space of the test tube with 5%H_2/95% N_2 mixed gas several times using the anaerobic chamber (Coy Laboratory Products, Inc). Oxic condition was performed by not purging the head-space, but leaving the space with atmospheric oxygen.

2.9. 1-Butanol quantification

Culture samples (1 ml) were centrifuged for 5 min at 21,130 × *g*. The supernatant (95 μL) was then mixed with 0.1% v/v 2-methyl-pentanol (5 μL) as internal standard. The mixture was then vortexed and directly analyzed on Agilent GC 6850 system with flame ionization detector and DB-FFAP capillary column (30 m, 0.32 mm i.d., 0.25 film thickness) from Agilent Technologies (Santa Clara, CA). 1-Butanol in the sample was identified and quantified by comparing to 0.001% v/v 1-butanol standard. 1-Butanol standard of 0.001% v/v was prepared by 100-fold dilution of a 0.1% v/v solution. The GC result was analyzed by Agilent software Chem Station (Rev.B.04.01 SP1). The amount of 1-butanol in the sample was then calculated based on the ratio of its integrated area and that of the 0.001% 1-butanol standard. 1-Butanol was verified by addition of 0.002% v/v butanol standard to the sample, showing complete overlap between butanol peak in the sample and the standard.

Helium gas was used as the carrier gas with 9.52 psi inlet pressure. The injector and detector temperatures were maintained at 225 °C. Injection volume was 1 μL. The GC oven temperature was initially held at 85 °C for 3 min and then raised to 235 °C with a temperature ramp of 45 °C/min. The GC oven was then maintained at 235 °C for 1 min before completion of analysis. Column flow rate was 1.7 ml/min. 1-Butanol typically had a retention time of 2.745 min. The internal standard 2-methyl-pentanol typically had a retention time of 3.945 min. The integrated area for the standard 0.001% v/v 1-butanol was usually about 3.36.

2.10. Preparation of cell extract for enzyme assays

For aerobic enzyme assays, the crude extract was obtained by pelleting 10 mL of cyanobacteria culture at OD_{730} of 1.5. The harvested cells were then resuspended in 3 mL of B-PERII (Thermo Scientific) solution mixed with lysonase™. After 10 min incubation, the solution was centrifuged. The supernatant was collected to use for enzyme assay. For the anoxic enzyme assays, similar procedure was followed with the exception of keeping samples in anoxic environment. Crude cell extract was prepared by centrifuging 5 mL of culture from anoxic production experiment in 4 °C for 20 min and resuspended the pellet in 1.5 mL of B-PERII with Lysonase™ and 5 mM DTT and incubated in room-temperature for 10 min in which the culture turned clear. The lysed cell extract was then centrifuged in 4 °C for 20 min to remove cell debris. The supernatant, containing soluble proteins, was used for enzyme assay. The protein concentration was determined by Bradford reagent using BSA as standards.

2.11. Thiolase (AtoB) assay

Thiolase activity was measured via the thiolysis direction. The enzymatic reaction was monitored by the decrease of absorbance at 303 nm, which corresponded to the result of acetoacetyl-CoA cleavage (Nishimura et al., 1978). The enzymatic reaction was initiated by the addition of the crude extract. The reaction mixture contained 100 mM Tris–HCl (pH 8.0), 10 mM $MgCl_2$, 200 μM acetoacetyl-CoA, and 200 μM CoA. The reaction temperature was at 30 °C.

2.12. 3-hydroxybutyryl-CoA dehydrogenase (Hbd) assay

Hbd activity was measured by monitoring the decrease in absorbance at 340 nm, which corresponded to consumption of NADH. The assay was conducted similar to previous reports (Boynton et al., 1996). The reaction mixture contained 100 mM MOPS (pH 7.0), 200 μM acetoacetyl-CoA, and 400 μM NADH. The reaction was initiated at the addition of crude extract.

2.13. Trans-2-enoyl-CoA reductase (Ter) assay

Ter activity was also measured by monitoring the decrease of absorbance at 340 nm similar to the Hbd assay. The assay was conducted similar to previous reports (Tucci and Martin, 2007) with slight modification. The mixture contained 100 mM potassium phosphate buffer (pH 6.2), 200 μM crotonyl-CoA, and 400 μM NADH.

2.14. Crotonase (Crt) assay

The Crt assay was conducted as described previously (Hartmanis and Gatenbeck, 1984) with minor modification. The assay reaction was monitored by a decrease of absorbance in 263 nm, corresponding to the disruption of the alpha–beta unsaturation of crotonyl-CoA. The assay mixture contained 100 mM Tris–HCl pH 7.6 and 200 μM Crotonyl-CoA. The reaction was initiated by addition of the enzyme. The standard curves of crotonyl-CoA and 3-hydroxybutyryl-CoA were constructed by measuring the absorbance of the two compounds at 263 nm with different concentrations. The difference in the molar absorptivity of the two compounds was used to calculate concentration of crotonyl-CoA.

2.15. Aldehyde/alcohol dehydrogenase assay

The aldehyde and alcohol dehydrogenase assay of AdhE2 was performed by monitoring the decrease of absorbance in 340 nm, corresponding to the consumption of NADH. The absorbance was monitored using Beckman-Coulter spectrophotometer DU-800. The reaction mixture contained 100 mM Tris–HCl pH 7.6, 5 mM DTT, 200 μM NADH, and 200 μM butyryl-CoA for the butyraldehyde dehydrogenase (Bldh) reaction and 10 mM butyraldehyde for the butanol dehydrogenase (Bdh) reaction. The total crude cell extract was used instead of only the soluble fraction. The reaction was initiated by the addition of the substrate (either butyryl-CoA or butyraldehyde). To determine the AdhE2 activity in anoxic condition, all procedure was performed in an anaerobic chamber with the exception of spectrophotometric measurement. The reaction was initiated in the anaerobic chamber. After thorough mixing, plastic cap was added onto the cuvette to prevent and reduce introduction of oxygen. The cuvette was then taken out of the anaerobic chamber and rapidly placed into spectrophotometer for kinetic measurement.

3. Results

3.1. Expression of 1-butanol pathway genes

The five genes required for 1-butanol production, *atoB*, *hbd*, *crt*, T.d-*ter*, and *adhE2*, were cloned into two separate plasmids, pEL5 and pEL14, designed for recombination at NSI (Bustos and Golden, 1992) and NSII (Andersson et al., 2000) of the *S. elongatus* 7942 genome (Table 2). Plasmid pEL5 targeted NSI and harbored *atoB* and *adhE2* under an IPTG inducible promoter, Ptrc, with spectinomycin as the antibiotic selection marker. Plasmid pEL14 targeted NSII and harbored *T.d-ter*, *crt*, and *hbd* under another IPTG

A

Strain	Modification on Ter	NSI	NSII	Ter activity (U/mg)	Butanol production (mg/L)
EL1	Original	Ptrc atoB adhE2	P_LlacO_1 T.d-ter crt hbd	0.0021	3.04±0.41
EL7	Codon optimized for *S. elongatus* 7942	Ptrc atoB adhE2	P_LlacO_1 $T.d\text{-}ter_{op}$ crt hbd	0.019	3.67±0.33
EL13	Gene rearrangement	Ptrc T.d-ter hbd crt	P_LlacO_1 atoB adhE2	0.057	11.58±0.58
EL14	Gene rearrangement + His-tag	Ptrc His-T.d-ter	P_LlacO_1 atoB adhE2 crt hbd	0.41	13.16±0.40

B

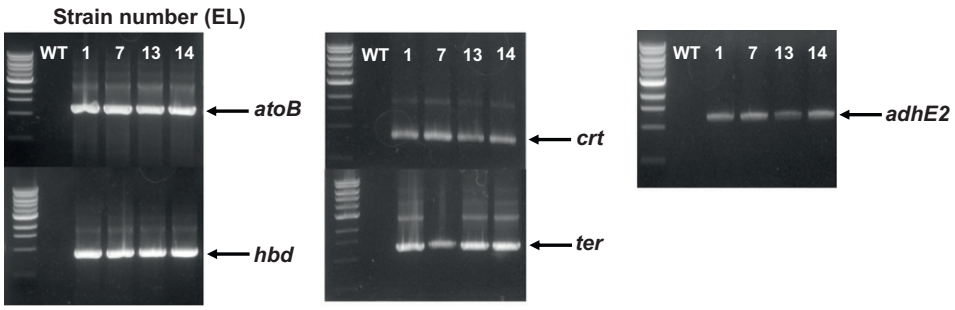

Fig. 2. (A) Schematics of gene arrangements in different strains that contain all of the 1-butanol production genes. Thiolase (*atoB*), aldehyde/alcohol dehydrogenase (*adhE2*), crotonase (*crt*), hydroxybutyryl-CoA dehydrogenase (*hbd*), trans-enoyl-CoA reductase (T.d-*ter*), codon optimized Ter (T.d-ter_{op}), and His-tagged Ter (His-*T.d-ter*). Error for Ter specific activity is listed in Table 4. One unit (U) is defined as μmol/min. (B) Whole cell PCR with gene-specific primers demonstrated the integration of each gene into the recombinant *S. elongatus* 7942 strains.

inducible promoter, $P_L lacO_1$, with kanamycin as the selection marker. The gene insertions (Fig. 2A) were then verified by whole cell colony PCR (Fig. 2B) of transformants obtained on antibiotic selection plates. The resulting recombinant strain EL1 (Fig. 2A) was cultured in liquid BG-11 medium for enzyme assay.

Crude extract of strain EL1 was assayed for each enzymatic reaction in the pathway. All enzyme activities were detected (Table 4). Specific activities of AdhE2 and Ter (Table 4) were two orders of magnitude lower than that of other enzymes in the pathway. The enzyme assay associated with AdhE2 has been previously conducted under anoxic condition (Fontaine et al., 2002; Vasconcelos et al., 1994), indicating its potential oxygen sensitivity. However *S. elongatus* 7942 generates oxygen during photosynthesis. Thus, AdhE2 within *S. elongatus* 7942 were expected to receive exposure of oxygen, which may have led to its reduction of activity. Therefore, we sought to investigate the potential oxygen sensitivity of AdhE2 by comparing its activities under oxic and anoxic conditions. The result (Table 5) of anoxic AdhE2 enzyme assay was consistent with the result obtained from the oxic assay, indicating that low AdhE2 activities were not completed due to oxygen sensitivity. Nevertheless, relative specific activities of AdhE2, to other enzymes, were comparable to that observed in *E. coli* (Table 4) by Shen et al. (2011). On the other hand, T.d-Ter activity, in contrast to the other enzymes, was significantly lower than expected when compared to previous *E. coli* results (Shen et al., 2011), which demonstrated T.d-Ter activity comparable to that of AtoB and Hbd in the high 1-butanol producing *E. coli* strain. Therefore these data suggested that T.d-Ter could be potential limiting steps for producing 1-butanol.

3.2. Improvement of Ter activity

To investigate the cause of low Ter activity, several approaches were taken. Ter homologs from *Treponema vincentii*, *Fibrobacter succinogenes*, *Flavobacterium johnsoniae, and E. gracilis* (Hoffmeister et al., 2005) have been identified based on sequence similarity with T.d-Ter. In particular, *E. gracilis* Ter (e.g. Ter) has been expressed in recombinant *E. coli* (Hoffmeister et al., 2005), indicating its potential for expression in other heterologous hosts. The two Ter homologs (from *T. denticola* and *E. gracilis*) were polyhistidine-tagged and expressed in *S. elongatus* 7942. His-*T.d-ter* and His-*E.g-ter* were separately cloned into two plasmids, pEL30 and pEL31, respectively. The two plasmids were then used to recombine the respective *ter* into wild-type *S. elongatus* 7942 at the NSI site. The resulting strains, EL9 with His-T.d-Ter and EL10 with His-E.g-Ter, were analyzed for their Ter expression by both Western blot and enzyme assay. Western blot (Fig. 3A) with His-tag specific probe showed expression of both His-T.d-Ter and His-E.g-Ter. The expression of His-T.d-Ter was higher than that of His-E.g-Ter as indicated by the thicker band in Western blot analysis (Fig. 3A). Furthermore, the expression of both His-T.d-Ter and His-E.g-Ter was analyzed by their *in vitro* activity (Fig. 3B). Interestingly, strain EL9, expressing His-T.d-Ter, showed Ter specific activity (0.444 μmol/min/mg) comparable to the activities of the other enzymes (Table 4) initially observed in strain EL1. This activity exceeded the Ter activity observed from EL1 by more than 100-fold. The His-E.g-Ter, on the other hand, demonstrated lower specific activity (0.065 μmol/min/mg) most likely due to less expression. The other genes of the pathway were then integrated into EL9 at NSII, resulting in strain EL14.

Simultaneously, we varied gene arrangement and optimized codon usage of T.d-*ter* for *S. elongatus* 7942, attempting to improve its activity or expression. Strain EL13 (Fig. 2A) contained every gene in the pathway at NSI under promoters Ptrc and $P_L lacO_1$. Strain EL7 (Fig. 2A) was constructed with the same gene configuration as strain EL1 with the substitution of *T.d-ter* with its codon-optimized version (T.d-ter_{op}). These strains were assayed for their enzyme activities from both oxic and anoxic incubated cultures (Tables 4 and 5). Ter activity was the highest in strain

Table 4
Enzymatic activities of different strains cultured oxygenically.

Enzyme	Strains					
	Wild-type	EL1	EL7	EL13	EL14	*E. coli*[a]
AtoB	n.d.	0.41 ± 0.02	0.20 ± 0.02	3.20 ± 1.0	0.18 ± 0.01	17 ± 2
Hbd	n.d.	0.27 ± 0.002	0.27 ± 0.06	0.29 ± 0.10	0.64 ± 0.29	4.6 ± 0.8
Crt	n.d.	7.92 ± 0.04	2.90 ± 1.3	2.90 ± 1.5	8.8 ± 4.6	97.9 ± 13.6
Ter	n.d.	0.0021 ± 0.0015	0.019 ± 0.002	0.057 ± 0.005	0.41 ± 0.25	3.7 ± 0.5
AdhE2 (Bldh)	n.d.	0.0042 ± 0.0010	0.0044 ± 0.0014	0.0034 ± 0.0010	0.0011 ± 0.0010	0.014 ± 0.001
AdhE2 (Bdh)	0.0021	0.0084 ± 0.0010	0.0086 ± 0.0010	0.0079 ± 0.0010	0.0031 ± 0.0010	0.007 ± 0.001

n.d. not detected. Specific activity is given in μmol/min/mg crude extract. AtoB, acetyl-CoA acetyltransferase; Hbd, 3-hydroxybutyryl-CoA dehydrogenase; Crt, crotonase; Ter, trans-2-enoyl-CoA reductase; Bldh, butyraldehyde dehydrogenase; and Bdh, butanol dehydrogenase.

[a] Data from Shen et al. (2011).

Table 5
Enzymatic activities of different strains after anoxic incubation.

Enzyme	Strain				
	Wild-type	EL1	EL7	EL13	EL14
AtoB	n.d.	0.46 ± 0.13	0.44 ± 0.18	4.71 ± 1.34	0.68 ± 0.19
Hbd	0.012 ± 0.005	0.31 ± 0.10	0.91 ± 0.22	1.08 ± 0.22	0.91 ± 0.16
Crt	n.d.	9.79 ± 3.49	26.56 ± 9.76	35.71 ± 9.63	17.06 ± 4.43
Ter	n.d.	0.017 ± 0.005	0.023 ± 0.006	0.18 ± 0.06	1.12 ± 0.22
AdhE2 (Bldh)	n.d.	0.0054 ± 0.0050	0.0048 ± 0.0040	0.0027 ± 0.0033	0.0010 ± 0.0016
AdhE2 (Bdh)	n.d.	0.0022 ± 0.0007	0.0023 ± 0.0004	0.0011 ± 0.0001	0.0003 ± 0.0001

n.d. not detected. Specific activity is given in μmol/min/mg crude extract. AtoB, acetyl-CoA acetyltransferase; Hbd, 3-hydroxybutyryl-CoA dehydrogenase; Crt, crotonase; Ter, trans-2-enoyl-CoA reductase; Bldh, butyraldehyde dehydrogenase; and Bdh, butanol dehydrogenase.

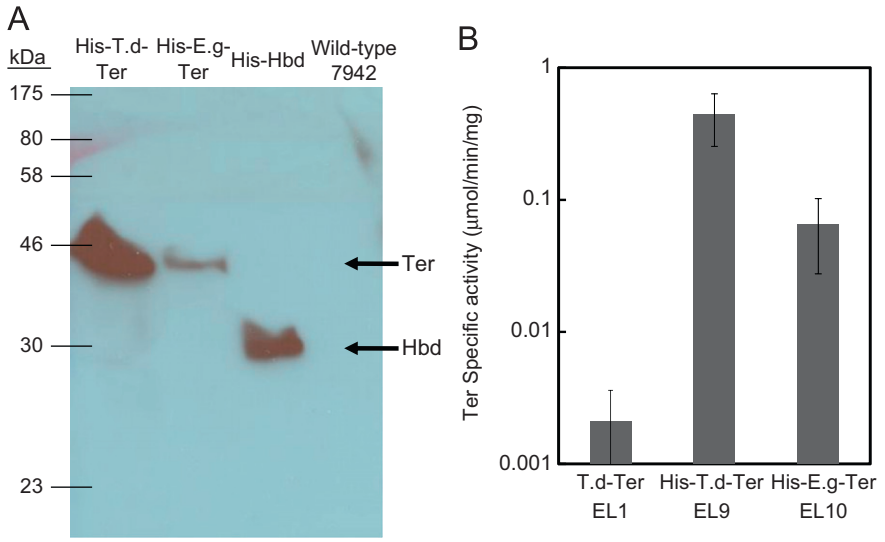

Fig. 3. Expression of His-tagged *T. denticola* and *E. gracilis* Ter demonstrated by enzymatic activity and western blot. (A) Analyzed protein samples were soluble fraction of crude extract from recombinant *S. elongatus* 7942 strains expressing individual enzymes. Lane 1, from the left, EL9 expressed His-tagged *T. denticola* Ter. Lane 2, EL10 expressed His-tagged *E. gracilis* Ter. Lane 3, EL11 expressed His-tagged *C. acetobutylicum Hbd*. Lane 4, crude extract from wild-type *S. elongatus* 7942, showing the absence of non-specific binding of the His-specific probe. (B) Ter specific activity of three different strains. In particular, strain EL9, expressing His-T.d-Ter, demonstrated the highest activity, which is more than 100-fold higher than that of strain EL1 that expressed T.d-Ter.

EL14 (Fig. 2A), which expressed His-T.d-Ter. Therefore strain EL14 was used as the potential production strain.

3.3. Dark anoxic incubation led to production of 1-butanol

Strain EL14 was tested for 1-butanol production under standard oxygenic incubation in constant light exposure. However, no 1-butanol production was observed both in screw-capped flasks and air-bubbling cultures. To test the effect of oxygen on the production of 1-butanol, we investigated different culturing conditions. Strain EL14 was grown under light with continuous bubbling of 5% CO_2 with 95% N_2 intended to remove oxygen from the culturing system. However, the effect seemed small as the culture accumulated only 2.2 mg/L (data not shown) of 1-butanol at the end of two weeks of growth. This result suggested that anoxic condition may aid butanol production in *S. elongatus* 7942. We then raised the question of perhaps bubbling CO_2/N_2 mixed gas was insufficient to remove oxygen generated from photosynthesis. Therefore, to further reduce oxygen exposure, a grown culture (OD_{730} of 4.3) of EL14 was incubated in dark anoxic condition (Fig. 4). 1-Butanol accumulation reached 14.5 mg/L in seven days while the cell density declined from OD_{730} of 3.9 to 2.4. This result suggested that the production of 1-butanol in *S. elongatus* 7942 is oxygen sensitive.

To test the effect of Ter activity on 1-butanol production, strains EL1, EL7, EL13, and EL14 (Fig. 2A) were incubated in the dark anoxic condition. Results (Fig. 2A) showed that EL14 and EL13 produced much better than EL1 and EL7. The production from these different recombinant strains positively correlated with their Ter activities (Table 5), indicating that this enzymatic step is important in the pathway. However, EL13 and EL14 produced comparable amount of 1-butanol while Ter activity of EL13 was about 10-fold lower than that of EL14. This result indicated that some other bottleneck exists in the pathway. Nevertheless, we demonstrated here that sufficient Ter activity more efficiently directs carbon flux to 1-butanol.

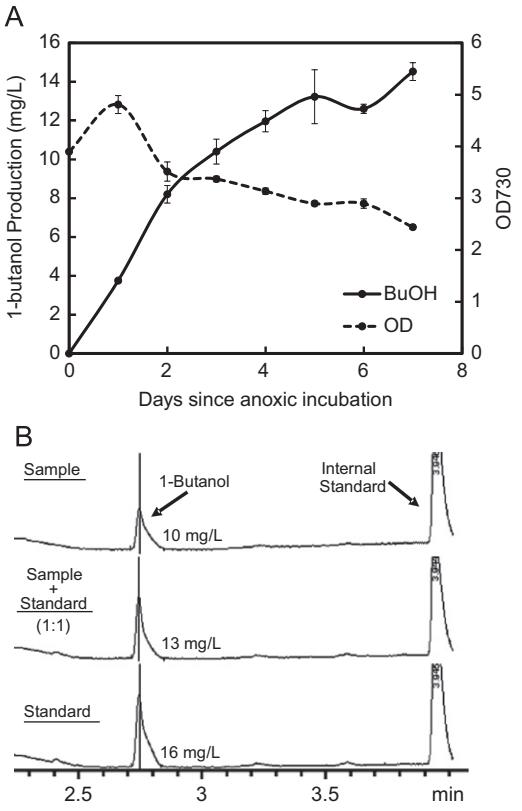

Fig. 4. 1-Butanol production from anoxically incubated strain EL14 in dark. 1-Butanol accumulated in culture medium to 14.5 mg/L with continuous decrease of cell density from OD_{730} of 3.9 to 2.4. The solid line represents 1-butanol accumulation. The dashed line represents cell density measured by OD_{730}. Error bars represent standard deviation of triplicate experiments. (B) GC measurement of 1-butanol accumulation in culture medium. Spiking the sample with 0.002% v/v butanol (1:1 volume ratio) showed complete overlap and consistent increment of 1-butanol peak. Internal standard used was 0.1% 2-methyl-pentanol.

3.4. Oxygen inhibits 1-butanol production

To further test the effect of oxygen, 3-(3,4-dichlorophenyl)-1,1-dimethylurea (DCMU) was used to inhibit photosystem II (PSII). DCMU blocks the plastoquinone binding site of PSII, efficiently inhibiting PSII's function and ability to generate oxygen under light. DCMU was added to both oxic and anoxic culture of strain EL14 in continuous light to test if oxygen inhibits the

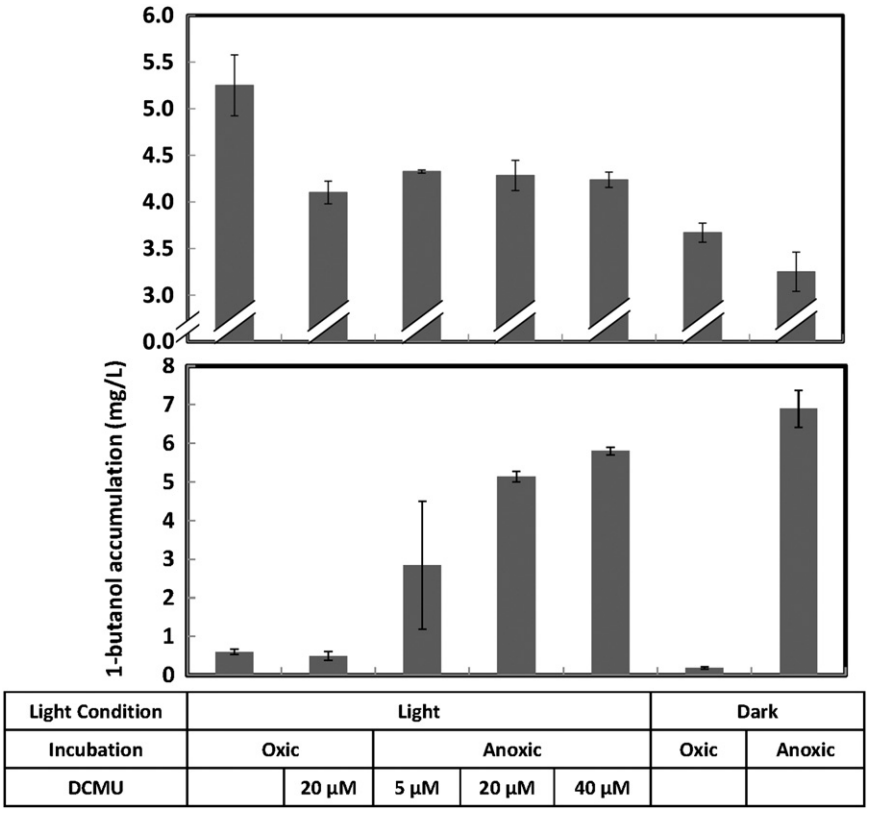

Fig. 5. Condition comparison for 1-butanol accumulation in recombinant cyanobacteria strain EL14. 1-Butanol accumulation was higher under anoxic condition. Amount of DCMU added had positive correlation with the amount of 1-butanol produced. Culture was incubated under various conditions after 2 weeks of growth in light with continuous bubbling of 5% CO_2 and 95% N_2 until OD_{730} of 4.3. Error bars represent standard deviation of triplicate experiments. Initial culture cell density was OD_{730} of 4.3.

1-butanol synthesis. If the lack of production in standard light oxygenic condition was due to light-induced regulation, rather than oxygen, then both light oxic and light anoxic cultures with DCMU would not produce 1-butanol. However, 1-butanol accumulated in the light anoxic culture with DCMU (Fig. 5), suggesting that oxygen, rather than light, inhibited the production. The amount of 1-butanol accumulated in the culture medium positively correlated with the amount of DCMU added (Fig. 5). This correlation indicated that 5 µM of DCMU only partially inhibited photosystem II, allowing the ability of the cells to produce small amounts of oxygen. The cell densities of these cultures remained constant for the 5-day period, maintaining at around OD_{730} of 4.3 (Fig. 5), indicating the ability of the cell to use photosystem I to maintain cellular functions. These results suggested that oxygen plays an important role in the production of 1-butanol in cyanobacteria. Elimination of oxygen was required for 1-butanol production.

4. Discussion

Production of chemicals and fuels from CO_2 is advantageous for reducing carbon emission as well as reducing reliance on petroleum. In this work, we achieved production of 1-butanol from CO_2 and light. Theoretically, at least 48 photons (Box 1) are required for producing one 1-butanol. This photon requirement is identical to that of glucose (Table 6). Thus, it is advantageous to produce 1-butanol directly from light rather than harvesting glucose and converting glucose to 1-butanol. The per photon value of 1-butanol (Table 6) is higher than that of sugar (Ducat et al., 2011).

Table 6
Photons required for producing desirable products.

Molecule	Molecular weight (g/mol)	Photon required	Cost/kg	Relative value/photon
Sugar [a]	180	48	0.5	1
Lactate [a]	90	24	1	2
1-Butanol	72	48	1.4[b]	1.12
Isobutanol	72	48	1.4[b]	1.12

[a] Calculation from Ducat et al. (2011).
[b] Average of values obtained from ICIS pricing (2010).

Among the CoA-dependent 1-butanol biosynthesis reactions, the crotonyl-CoA reduction has been previously (Atsumi et al., 2008a) identified as the limiting step in this pathway. Ter (Bond-Watts et al., 2011; Shen et al., 2011) has been demonstrated to outperform *Clostridium* Bcd–EtfAB complex by utilizing NADH as the direct reducing cofactor in effect forcing the reduction irreversible. In this work, we also observed that this step was a potential bottleneck, as insufficient Ter activity led to lower 1-butanol production. Interestingly, the overall activity of this enzyme was increased 100-fold by attaching a polyhistidine-tag to *T.d* Ter, and the 1-butanol production increased about 5-fold. N-terminus His-tag has been previously (Doray et al., 2001) shown to increase expression of enzymes. We attributed the Ter activity increase to a similar phenomenon. This result highlights the possibility of using protein fusion as a way to improve expression in metabolic engineering work. In *E. coli*, Shen et al. (2011) further increase the metabolic driving force by artificially building up NADH and acetyl-coA availability. Such efforts are expected to improve 1-butanol production in cyanobacteria as well.

Absence of oxygen is an important factor in the production of 1-butanol in cyanobacteria. While AdhE2 has been purified and assayed only in anoxic atmosphere (Fontaine et al., 2002), suggesting its oxygen sensitivity, we were able to detect comparable AdhE2 activities both under oxic and anoxic conditions. Therefore, it is unclear whether the potential oxygen-sensitivity of AdhE2 is the limitation for oxygenic production of 1-butanol. Other factors such as cofactor availability may contribute to the anoxic requirement of 1-butanol production.

In this study, the internal storage of reduced carbon compounds in cyanobacteria is directed to 1-butanol pathway under anoxic condition. This production system could be suitable and even advantageous for natural light cycles. In day time, cyanobacteria accumulate internal storage reduced carbon. At night, when light energy is not available, cyanobacteria produce 1-butanol after removal of oxygen in the system. This system could be optimized by increasing storage of reduced carbon. The production described here is similar to that of hydrogen production in cyanobacteria and algae (Antal et al., 2003; Melis et al., 2000), which also involves inhibition of photosystem II once entering production phase due to the oxygen sensitivity nature of hydrogenases.

The high flux production of isobutyraldehyde and isobutanol (Atsumi et al., 2009) demonstrates that high efficiency conversion of solar energy into desirable compounds is feasible. Having the same 48 photon requirement as isobutanol, 1-butanol production has the potential for improvement. For example, expression of an NAD(P) transhydrogenase, such as *E. coli* UdhA or PntAB, will interconvert NADH and NADPH. This approach is beneficial for production because NADH is the cofactor required by this pathway. In addition, changing the enzyme cofactor dependence from NADH to NADPH either by bio-prospecting for enzymes that naturally use NADPH or by protein engineering methods (Scrutton et al., 1990) would also compensate the cofactor discrepancy. For example, enzymes such as acetoacetyl-CoA reductase (PhaB) (Peoples and Sinskey, 1989) from *Ralstonia eutropha* and crotonyl-CoA reductase (Ccr) (Wallace et al., 1995) from *Streptomyces collinus* use NADPH as the reducing agent to catalyze similar reactions as Hbd and Ter, respectively.

As an alternative, purple or green sulfur bacteria may be engineered with this pathway to avoid oxygen sensitivity. Purple and green sulfur bacteria are anaerobes or microaerobes that perform anoxygenic photosynthesis by utilizing hydrogen sulfide as electron donor. In these organisms, production of 1-butanol would not depend on internal storage of reduced carbon. Instead, they may directly convert CO_2 into 1-butanol.

Acknowledgment

This work was supported by The Kaiteki Institute, Japan. J.C.L. was partially supported by the UCLA-DOE Institute of Genomics and Proteomics. The authors would like to thank Dr. Hao Luo, Dr. Hidevaldo, B. Machado, Dr. Kwang Myung Cho, Claire R. Shen, and Yasumasa Dekishima for their technical assistance as well as intriguing discussions.

Appendix A. Supplementary data

Supplementary data associated with this article can be found in the online version at doi:10.1016/j.ymben.2011.04.004.

References

Andersson, C.R., Tsinoremas, N.F., Shelton, J., Lebedeva, N.V., Yarrow, J., Min, H.T., Golden, S.S., 2000. Application of bioluminescence to the study of circadian rhythms in cyanobacteria. Biolumin. Chemilumin., Pt. C 305, 527–542.

Antal, T.K., Krendeleva, T.E., Laurinavichene, T.V., Makarova, V.V., Ghirardi, M.L., Rubin, A.B., Tsygankov, A.A., Seibert, M., 2003. The dependence of algal H_2 production on photosystem II and O_2 consumption activities in sulfur-deprived *Chlamydomonas reinhardtii* cells. Biochim. Biophys. Acta 1607, 153–160.

Atsumi, S., Cann, A.F., Connor, M.R., Shen, C.R., Smith, K.M., Brynildsen, M.P., Chou, K.J.Y., Hanai, T., Liao, J.C., 2008a. Metabolic engineering of *Escherichia coli* for 1-butanol production. Metab. Eng. 10, 305–311.

Atsumi, S., Hanai, T., Liao, J.C., 2008b. Non-fermentative pathways for synthesis of branched-chain higher alcohols as biofuels. Nature 451, 86–89.

Atsumi, S., Higashide, W., Liao, J.C., 2009. Direct photosynthetic recycling of carbon dioxide to isobutyraldehyde. Nat. Biotechnol. 27, 1177–1180.

Atsumi, S., Liao, J.C., 2008. Metabolic engineering for advanced biofuels production from *Escherichia coli*. Curr. Opin. Biotechnol. 19, 414–419.

Berezina, O.V., Zakharova, N.V., Brandt, A., Yarotsky, S.V., Schwarz, W.H., Zverlov, V.V., 2010. Reconstructing the clostridial n-butanol metabolic pathway in *Lactobacillus brevis*. Appl. Microbiol. Biotechnol. 87, 635–646.

Bond-Watts, B.B., Bellerose, R.J., Chang, M.C.Y., 2011. Enzyme mechanism as a kinetic control element for designing synthetic biofuel pathways. Nat. Chem. Biol. 7, 222–227.

Boynton, Z.L., Bennett, G.N., Rudolph, F.B., 1996. Cloning, sequencing, and expression of clustered genes encoding beta-hydroxybutyryl-coenzyme A (CoA) dehydrogenase, crotonase, and butyryl-CoA dehydrogenase from *Clostridium acetobutylicum* ATCC 824. J. Bacteriol. 178, 3015–3024.

Brenner, M.P., et al., 2008. Engineering Microorganisms for Energy Production. U.S. Department of Energy, Washington, DC.

Bustos, S.A., Golden, S.S., 1991. Expression of the Psbdii Gene in *Synechococcus* Sp Strain-Pcc-7942 requires sequences downstream of the transcription start site. J. Bacteriol. 173, 7525–7533.

Bustos, S.A., Golden, S.S., 1992. Light-regulated expression of the Psbd gene family in *Synechococcus*-Sp Strain Pcc-7942—evidence for the role of duplicated Psbd genes in cyanobacteria. Mol. Gen. Genet. 232, 221–230.

Deng, M.D., Coleman, J.R., 1999. Ethanol synthesis by genetic engineering in cyanobacteria. Appl. Environ. Microbiol. 65, 523–528.

Dexter, J., Fu, P.C., 2009. Metabolic engineering of cyanobacteria for ethanol production. Energy Environ. Sci. 2, 857–864.

Doray, B., Chen, C.D., Kemper, B., 2001. N-terminal deletions and His-tag fusions dramatically affect expression of cytochrome p450 2C2 in bacteria. Arch. Biochem. Biophys. 393, 143–153.

Ducat, D.C., Way, J.C., Silver, P.A., 2011. Engineering cyanobacteria to generate high-value products. Trends Biotechnol.

Duncombe, G.R., Frerman, F.E., 1976. Molecular and catalytic properties of acetoacetyl-coenzyme-a thiolase of *Escherichia-Coli*. Arch. Biochem. Biophys. 176, 159–170.

Ezeji, T.C., Qureshi, N., Blaschek, H.P., 2004. Butanol fermentation research: upstream and downstream manipulations. Chem. Rec. 4, 305–314.

Fischer, C.R., Klein-Marcuschamer, D., Stephanopoulos, G., 2008. Selection and optimization of microbial hosts for biofuels production. Metab. Eng. 10, 295–304.

Fontaine, L., Meynial-Salles, I., Girbal, L., Yang, X.H., Croux, C., Soucaille, P., 2002. Molecular characterization and transcriptional analysis of adhE2, the gene encoding the NADH-dependent aldehyde/alcohol dehydrogenase responsible for butanol production in alcohologenic cultures of *Clostridium acetobutylicum* ATCC 824. J. Bacteriol. 184, 821–830.

Gibson, D.G., Young, L., Chuang, R.Y., Venter, J.C., Hutchison, C.A., Smith, H.O., 2009. Enzymatic assembly of DNA molecules up to several hundred kilobases. Nat. Methods 6, 343–345.

Hanai, T., Atsumi, S., Liao, J.C., 2007. Engineered synthetic pathway for isopropanol production in *Escherichia coli*. Appl. Environ. Microbiol. 73, 7814–7818.

Hartmanis, M.G.N., Gatenbeck, S., 1984. Intermediary metabolism in *Clostridium-Acetobutylicum*—levels of enzymes involved in the formation of acetate and butyrate. Appl. Environ. Microbiol. 47, 1277–1283.

Hoffmeister, M., Piotrowski, M., Nowitzki, U., Martin, W., 2005. Mitochondrial trans-2-enoyl-CoA reductase of wax ester fermentation from *Euglena gracilis* defines a new family of enzymes involved in lipid synthesis. J. Biol. Chem. 280, 4329–4338.

Inui, M., Suda, M., Kimura, S., Yasuda, K., Suzuki, H., Toda, H., Yamamoto, S., Okino, S., Suzuki, N., Yukawa, H., 2008. Expression of *Clostridium acetobutylicum* butanol synthetic genes in *Escherichia coli*. Appl. Microbiol. Biotechnol. 77, 1305–1316.

Jiang, Y., Xu, C., Dong, F., Yang, Y., Jiang, W., Yang, S., 2009. Disruption of the acetoacetate decarboxylase gene in solvent-producing *Clostridium acetobutylicum* increases the butanol ratio. Metab. Eng. 11, 284–291.

Li, F., Hinderberger, J., Seedorf, H., Zhang, J., Buckel, W., Thauer, R.K., 2008. Coupled ferredoxin and crotonyl coenzyme a (CoA) reduction with NADH catalyzed by the butyryl-CoA dehydrogenase/Etf complex from *Clostridium kluyveri*. J. Bacteriol. 190, 843–850.

Lin, Y.L., Blaschek, H.P., 1983. Butanol production by a butanol-tolerant strain of *Clostridium-Acetobutylicum* in extruded corn broth. Appl. Environ. Microbiol. 45, 966–973.

Lindberg, P., Park, S., Melis, A., 2010. Engineering a platform for photosynthetic isoprene production in cyanobacteria, using *Synechocystis* as the model organism. Metab. Eng. 12, 70–79.

Melis, A., Zhang, L.P., Forestier, M., Ghirardi, M.L., Seibert, M., 2000. Sustained photobiological hydrogen gas production upon reversible inactivation of oxygen evolution in the green alga *Chlamydomonas reinhardtii*. Plant Physiol. 122, 127–135.

Nicolaou, S.A., Gaida, S.M., Papoutsakis, E.T., 2010. A comparative view of metabolite and substrate stress and tolerance in microbial bioprocessing: from biofuels and chemicals, to biocatalysis and bioremediation. Metab. Eng. 12, 307–331.

Niederholtmeyer, H., Wolfstadter, B.T., Savage, D.F., Silver, P.A., Way, J.C., 2010. Engineering cyanobacteria to synthesize and export hydrophilic products. Appl. Environ. Microbiol. 76, 3462–3466.

Nielsen, D.R., Leonard, E., Yoon, S.H., Tseng, H.C., Yuan, C., Prather, K.L.J., 2009. Engineering alternative butanol production platforms in heterologous bacteria. Metab. Eng. 11, 262–273.

Nishimura, T., Saito, T., Tomita, K., 1978. Purification and properties of beta-ketothiolase from *Zoogloea ramigera*. Arch. Microbiol. 116, 21–27.

Peoples, O.P., Sinskey, A.J., 1989. Poly-beta-hydroxybutyrate (Phb) biosynthesis in Alcaligenes-Eutrophus H16—identification and characterization of the Phb polymerase gene (Phbc). J. Biol. Chem 264, 15298–15303.

Scrutton, N.S., Berry, A., Perham, R.N., 1990. Redesign of the coenzyme specificity of a dehydrogenase by protein engineering. Nature 343, 38–43.

Sheehan, J., 2009. Engineering direct conversion of CO_2 to biofuel. Nat. Biotech. 27, 1128–1129.

Shen, C.R., Lan, E.I., Dekishima, Y., Baez, A., Cho, K.M., Liao, J.C., 2011. High titer anaerobic 1-butanol synthesis in *Escherichia coli* enabled by driving forces. Appl. Environ. Microbiol.

Shen, C.R., Liao, J.C., 2008. Metabolic engineering of *Escherichia coli* for 1-butanol and 1-propanol production via the keto-acid pathways. Metab. Eng. 10, 312–320.

Sillers, R., Chow, A., Tracy, B., Papoutsakis, E.T., 2008. Metabolic engineering of the non-sporulating, non-solventogenic *Clostridium acetobutylicum* strain M5 to produce butanol without acetone demonstrate the robustness of the acid-formation pathways and the importance of the electron balance. Metab. Eng. 10, 321–332.

Steen, E.J., Chan, R., Prasad, N., Myers, S., Petzold, C.J., Redding, A., Ouellet, M., Keasling, J.D., 2008. Metabolic engineering of *Saccharomyces cerevisiae* for the production of n-butanol. Microb. Cell Fact., 7.

Takahama, K., Matsuoka, M., Nagahama, K., Ogawa, T., 2003. Construction and analysis of a recombinant cyanobacterium expressing a chromosomally inserted gene for an ethylene-forming enzyme at the psbAI locus. J. Biosci. Bioeng. 95, 302–305.

Tucci, S., Martin, W., 2007. A novel prokaryotic trans-2-enoyl-CoA reductase from the spirochete *Treponema denticola*. FEBS Lett. 581, 1561–1566.

Vasconcelos, I., Girbal, L., Soucaille, P., 1994. Regulation of carbon and electron flow in *Clostridium-acetobutylicum* grown in chemostat culture at neutral PH on mixtures of glucose and glycerol. J. Bacteriol. 176, 1443–1450.

Wallace, K.K., Bao, Z.Y., Dai, H., Digate, R., Schuler, G., Speedie, M.K., Reynolds, K.A., 1995. Purification of crotonyl-CoA reductase from *Streptomyces collinus* and cloning, sequencing and expression of the corresponding gene in *Escherichia coli*. Eur. J. Biochem. 233, 954–962.

Wiesenborn, D.P., Rudolph, F.B., Papoutsakis, E.T., 1988. Thiolase from *Clostridium-acetobutylicum* Atcc-824 and its role in the synthesis of acids and solvents. Appl. Environ. Microbiol. 54, 2717–2722.

Zhang, K., Sawaya, M.R., Eisenberg, D.S., Liao, J.C., 2008. Expanding metabolism for biosynthesis of nonnatural alcohols. Proc. Natl. Acad. Sci. USA 105, 20653–20658.

Zhu, X.G., Long, S.P., Ort, D.R., 2008. What is the maximum efficiency with which photosynthesis can convert solar energy into biomass? Curr. Opin. Biotechnol. 19, 153–159.